

The major histocompatibility complex class I immunopeptidome of extracellular vesicles.

Silvia A. Synowsky¹, Sally L. Shirran¹, Fiona G. M. Cooke², Antony N. Antoniou³, Catherine H. Botting¹ and Simon J. Powis^{2*}.

1. Biomedical Sciences Research Complex, University of St Andrews, St Andrews, KY16 9ST, UK.
2. School of Medicine, University of St Andrews, St Andrews, KY16 9TF, UK.
3. The Advanced Centre for Biochemical Engineering, University College London, London, WC1E 7JE.

Running title: The immunopeptidome of extracellular vesicles

* To whom correspondence should be addressed: Simon Powis, School of Medicine, University of St Andrews, St Andrews, KY16 9TF, UK. Email: sjp10@st-andrews.ac.uk

Key words: antigen presentation, extracellular vesicles, MHC class I.

Abstract.

Extracellular vesicles (EVs) are released by most cell types and have been associated with multiple immunomodulatory functions. MHC class I molecules have crucial roles in antigen presentation and in eliciting immune responses and are known to be incorporated into EVs. However, the MHC class I immunopeptidome of EVs has not been established. Here, using a small-scale immunoisolation of the antigen serotypes HLA-A*02:01 and HLA-B*27:05 expressed on the Epstein–Barr virus–transformed B cell line Jethom and MS of the eluted peptides from both cells and EVs, we identified 516 peptides that bind either HLA-A*02:01 or HLA-B*27:05. Of importance, the predicted serotype-binding affinities and peptide-anchor motifs did not significantly differ between the peptide pools isolated from cells or EVs, indicating that during EV biogenesis, no obvious editing of the MHC class I immunopeptidome occurs. These results, for the first time, establish EVs as a source of MHC class I peptides that can be used for the study of the immunopeptidome and in the discovery of potential neoantigens for immunotherapies.

Introduction.

Extracellular vesicles (EVs), including those known as exosomes, are released by many types of cells, and have been ascribed numerous functions in cellular communication, including the propagation of niche sites for tumour metastases (1), facilitating viral infection (2) and in

angiogenesis (3), amongst many others. EVs are thought to originate from multivesicular bodies and are secreted following fusion of multivesicular bodies (MVB) with the plasma membrane (4,5).

Within the immune system EVs have been reported to have mostly immunoinhibitory functions (6), although dendritic cell- and tumour cell-derived EVs have shown some promise in the stimulation of anti-tumour responses (7). EVs have also been demonstrated to have a role in transplantation responses, leading to a reassessment of the passenger leukocyte hypothesis (8) and have been demonstrated to influence thymic selection (9). These physiological and therapeutic roles in the immune system imply that peptide presentation by Major Histocompatibility Complex (MHC) molecules on EVs have a profound effect on their role in eliciting immune responses. To date, no information exists on the peptide repertoire that is presented by EVs. MHC expression and peptide presentation by EVs could be an important determining factor for their general effectiveness, as they could modulate EV-immune cell interactions, which potentially may affect their therapeutic value.

In relation to the Major Histocompatibility Complex (MHC) class I system proteins and their role as antigen presenting molecules to CD8⁺ T cells, we have previously shown that MHC class I molecules are incorporated into EVs from a number of cell lines, including the Jethom line used in the current study (10–12). However, their ability to modulate CD8⁺ activity has not been studied in detail,

although EVs loaded exogenously with common immunogenic viral peptides can stimulate IFN γ and TNF α release from purified human CD8 $^+$ T cells, indicating EVs can directly impact on the behaviour of these cells (13).

In order to further understand the role of MHC class I on EVs we have undertaken here to determine their immunopeptidome, i.e. the repertoire of the peptides being presented. The null hypothesis would be that the EV pool of MHC class I bound peptides would be an exact copy of those present on the cell surface. However, since EVs can be derived from an endocytic route involving the formation of MVB, editing of the peptide repertoire could occur, by dissociation of weak affinity peptides and/or loading of peptides from within the MVB compartment, thus generating potential EV-associated neoantigens. This could be of significant importance in the search for novel MHC class I epitopes and development of patient-tailored immunotherapies.

In this study we have performed small scale MHC class I immunoisolation and peptide extraction to determine the repertoire of peptides from EVs of the EBV-transformed B cell line Jesthom, providing the first data that EVs can be used as a source for immunopeptidomic studies of MHC class I epitopes in health and disease.

Results

The EBV-transformed B cell line Jesthom expresses HLA-A*02:01 and HLA-B*27:05. Three small-scale immunoisolation experiments were performed from approximately 250, 600 and 800 million Jesthom cells, yielding approximately 200, 300 and 400 μ g of EVs respectively. Importantly, cell lysates and EVs from the same culture were processed concomitantly to prevent temporal sample variations due to dissociation of low affinity peptides. EVs were isolated by standard procedures of filtration and ultracentrifugation. Immunoblot analysis of a sample of the cell and EV lysates indicated enrichment of MHC class I, and the prototypical EV markers CD9 and CD81 in the EV isolates, whereas the non-EV marker GRP78 (BiP) was present at very low levels in EVs (Figure 1A). From a series of cultures with approximately 10 million Jesthom cells, the enrichment of HLA-A

molecules and HLA-B molecules in EV was between 1.8 and two-fold (Supplementary Figure 1). Nanoparticle tracking analysis (NTA), which utilises light scattering of particles in suspension undergoing Brownian motion, of culture supernatant after 0.2 μ m filtration, but prior to ultracentrifugation indicated three typical peaks of around 61, 86 and 142 nm (Figure 1B), with a mean of 151 nm and mode of 115 nm from three preparations. The samples therefore represent typical EVs. From a separate test run of 400 million Jesthom cells, an estimated concentration of 400×10^9 particles were detected by NTA, indicating the release of approximately 1,000 EV per cell over the course of 48 hours.

The cell and EV lysates were immunoisolated with the anti-HLA-A, -B and -C mAb W6/32, pre-absorbed (but not cross-linked) to Protein-G agarose beads. After extensive washing, 2% of the beads were removed and analysed by SDS-PAGE and Coomassie blue staining or immunoblotting with the anti-HLA-B and -C specific mAb HC10. Compared to the control W6/32 (no lysate) sample additional bands at approximately 43 kDa were detected in both cell and EV samples (Figure 1C), which were HC10 reactive (Figure 1D). Additional bands were detected migrating at the dye front, which were presumed to be β 2-microglobulin (Figure 1C). The remaining 98% of the immunoisolated cell and EV samples were acidified in 0.5% TFA to denature the MHC class I molecules, and the low molecular mass peptide pool fraction isolated with Centricon 3 centrifugal filters. The isolated peptide fraction was then processed and analysed by mass spectrometry.

Identified peptides from the resulting MASCOT files between 8 and 13 amino acids long were analysed for HLA-A*02:01 and HLA-B*27:05 predicted binding affinity using the NetMHCcons 1.1 server, which combines three algorithms (NetMHC, NetMHCpan and PickPocket). From the combined data of the three biological replicates 145 and 94 peptides were identified from HLA-B*27:05 cell and EV preparations respectively, and 172 and 105 peptides from HLA-A*02:01 cell and EV preparations respectively (Table 1 and Supplementary Table 1). In addition eleven HLA-C*01:02

(also expressed by Jesthom cells) peptides were also identified but are not reported here due to low numbers. The mean predicted binding affinity of the HLA-A*02:01 binding peptide pool was 33.3 nM for cells and 26.7 nM for EVs (Figure 2A), and for the HLA-B*27:05 binding peptide pool the mean predicted affinity was 225.9 nM for cells and 199.5 nM for EVs (Figure 2C). Whilst this might suggest that there is a loss of some lower affinity peptides during the biogenesis of EVs, two tailed Mann Whitney tests indicated no significant differences between the cell and EV pools for either MHC class I allele (HLA-A*02:01, $P = 0.8329$ and HLA-B*27:05, $P = 0.3199$ respectively). Peptide lengths did not alter, with a predominance of 9 mer peptides in both cells and EV for both HLA-A*02:01 and HLA-B*27:05 (Figure 2B and D). The anchor binding motifs were also analysed by Seq2logo for 9, 10 and 11 mer peptide pools from each source, with no significant alterations between the typical P2 Leu and C-terminal Val/Leu anchors for HLA-A*02:01 (Figure 2E) and the P2 Arg and C-terminal Phe/Tyr anchors for HLA-B*27:05 (Figure 2F). 26 of the 94 HLA-B*27:05 peptides in the EV pool were not detected in the cell-derived pool, and 34 of the 105 HLA-A*02:01 peptides from EVs were not detected in the cell-derived pool (highlighted in red in Table 1), however the cellular origin of these peptides was mostly from the cytoplasm and nucleus, suggesting they would also appear in the cell derived pool in a larger sample size. One HLA-A*02:01 binding peptide (LLLDVPTAAV) was identified from the endosome-located thiol-reductase GILT, but this has previously been reported in cells and therefore unlikely to be EV-specific (14). Taken together the data indicates that the MHC class I immunopeptidome of EVs is a replica of that found on the cell surface.

Discussion.

Our data has several important implications. It demonstrates that the EV immunopeptidome is essentially identical to that of the cell of origin. As such, important antigenic peptides, such as viral or tumour associated antigens (TAA) and tumour specific antigens (TSA) are likely to be released in EVs, potentially subverting antigen specific CD8⁺ cytotoxic T cells at a

distance from the infected cell or main tumour, thus potentially reducing effective CTL responses. The same observation would however also imply that EVs can be used as an effective source to isolate and detect TSA and TAA from readily available biological samples such as blood. EVs are known to be raised in pathological conditions (15,16), suggesting a relatively non-invasive technique for screening. As such, the EV-derived peptidome can now be studied as a source for neoantigens for personalised immunotherapeutic approaches, as recently demonstrated in principle for melanoma solid tissue biopsies (17). Such identified peptides could then be utilised in dendritic cell exosome (DEX) based therapies (18), for which phase I and II trials have already been conducted. Furthermore this MS technique could be used to monitor the efficacy of target-peptide loading onto DEX.

Our study does have some limitations. Our current small-scale study yielded a few hundred peptides, but larger samples and improved detection could yield thousands of identified peptides. The small, but consistent alteration in predicted binding affinities in the EV peptide pool would be worth studying in greater detail with such larger sample sizes. The residency time of an MHC class I complex during its incorporation into and secretion via an EV would be expected to promote the loss of low affinity peptides. Larger sample sizes would help resolve this issue. Furthermore, variations in the biogenesis of MVBs in different cell types could also have a significant impact upon the EV immunopeptidome. An extensive study of multiple cell types is now required. Of technical interest the antibody based immunoisolation of MHC molecules for peptide isolation utilised here is just one of several possible techniques (19). We have also performed preliminary studies on EV samples using mild acid elution (MAE), which in theory would not disrupt the cell or EV samples. The MAE technique removes the detergent lysis, immunoisolation and extensive washing steps that could lead to loss of low affinity peptides. However, MAE is known to produce increased peptide signals of non-MHC origin (20), but intriguingly we were able to detect some peptides with known binding motifs for the MHC class II molecules expressed on Jesthom cells (data

not shown), thus further enhancing the capacity of EVs to produce useful immunopeptidomic information. Taken together our study opens a new avenue for the characterisation of the immunopeptidome from highly biologically relevant vesicles.

Experimental Procedures.

Cell and EV isolation.

The EBV transformed B cell line (obtained from European Collection of Authenticated cell Lines no. 88052004) was grown in RPMI 1640 (Invitrogen, UK) supplemented with 5% FBS (Invitrogen, UK). Once the required number of cells was obtained, the medium was replaced with serum free medium to prevent contamination from FBS derived exosomes (EX-Cell 610-HSF serum free, Sigma-Aldrich, UK) for 48 hours. Cells were then isolated by centrifugation (300 x g, 10 min). The cells were washed once in PBS, then immediately resuspended in 5 ml lysis buffer (1% NP40, 150 mM NaCl, 10 mM Tris pH 7.6, with 1 mM PMSF). After 10 min on ice the lysates were centrifuged at 20,000 x g for 5 min and the supernatant stored on ice. 10-20 μ l was removed for immunoblotting. The EV containing supernatant was processed immediately by 0.2 μ m filtration and ultracentrifugation at 100,000 x g for 2 hours. The pellets were resuspended in 500 μ l PBS and 10-20 μ l removed for BCA protein estimation or EV characterisation by immunoblotting. The remaining bulk EV suspension was immediately lysed in 5 ml lysis buffer, as above.

EV characterisation.

Nanoparticle tracking analysis was performed on a 0.5 ml cell culture sample after 0.2 μ m filtration. Videos were taken using a Nanosight LM-10 unit (Malvern, UK), with 4 ms camera shutter and analysis detection threshold of 2 using NTA 2.3 software. For immunoblotting, 5 μ g of cell or EV lysates were run on 4-20% gels (Invitrogen) and transferred to nitrocellulose. Samples were incubated with the following antibodies overnight, HC10 (anti-HLA-B and -C), HCA2 (anti-HLA-A, a gift from Jacques Neefjes, Leiden), anti-GRP78 (dilution 1:5000, code: STJ97526 St Johns Laboratories, UK), or anti-CD9 or -CD81 (ThermoFisher Scientific UK, codes: anti-

CD9 clone Ts9, dilution 1:5000, code 15328354, CD81, dilution 1:5000, code 15304032). Immunoblots were then incubated with 1:10,000 diluted IR Dye800cw anti-mouse IgG (Licor, UK, code 925-32210) and visualised using a Licor Odyssey scanner.

Immunoisolation of MHC class I peptides.

0.5 ml of Protein G -agarose (code 20399, binding capacity 11-15 mg/ml IgG, ThermoScientific UK) were pre-loaded with 30 ml of W6/32 containing tissue culture supernatant for 20 min at room temperature, then washed twice in lysis buffer. The beads were then added to the cell and EV lysates and mixed for 1 hour at 4°C. Control W6/32 loaded beads received lysis buffer alone. The beads were then washed with 60 volumes (3x 10 ml) of lysis buffer without NP40. 10 μ l of beads was then removed for reducing SDS-PAGE and Coomassie blue staining (Gelcode Blue, ThermoScientific, UK). The remaining beads were resuspended in 1 ml 0.5 % TFA for 10 min at room temperature. The supernatant was then spun at 12,000 x g through pre-washed (in 0.1 % TFA) Centricon 3 filtration units (MerckMillipore, UK). The peptide containing flow through was then stored at -20°C until analysis by mass spectrometry.

Mass spectrometry.

Peptides were concentrated using a C18 column (NEST, ThermoScientific UK), eluted in 70% ACN/0.5% TFA and dried down by Speed Vac. Peptides were then analysed on an AB Sciex TripleTOF 5600+ system mass spectrometer (Sciex, Framingham, MA, USA) coupled to an Eksigent nanoLC AS-2/2Dplus system. The samples were loaded in loading buffer (2% acetonitrile and 0.05% trifluoroacetic acid) and bound to an Aclaim pepmap 100 μ m x 2 cm trap (Thermo Fisher Scientific), and washed for 10 min to waste after which the trap was turned in-line with the analytical column (Aclaim pepmap RSLC 75 μ m x 15 cm). The analytical solvent system consisted of buffer A (2% acetonitrile and 0.1% formic acid in water) and buffer B (2% water with 0.1% formic acid in acetonitrile) at a flow rate of 300 nl/min with the following gradient: linear 1-20% of buffer B over 90 min, linear 20-40% of buffer B for 30 min, linear 40-99% of buffer B for 10 min, isocratic 99% of

buffer B for 5 min, linear 99-1% of buffer B for 2.5 min and isocratic 1% solvent buffer B for 12.5 min. The mass spectrometer was operated in DDA top 20 positive ion mode, with 120 ms and 80 ms acquisition time for the MS1 (m/z 400-1250) and MS2 (m/z 95-1800) scans respectively, and 15 s dynamic exclusion. Rolling collision energy was used for fragmentation. Peak lists were generated within PeakView by using the “create mgf file” script. MASCOT search engine with the following search parameters was used to identify peptides: no enzyme specificity, maximum of 4 miscleavages, oxidation as variable modification, peptide tolerance was set to 20 ppm and the MSMS tolerance to 0.1Da. Data was searched against Swiss Prot database downloaded November 2016, restricted to proteins from humans only.

Peptides identified in the Mascot files were assessed for their potential allele binding specificity and affinity using the NetMHCcons 1.1 algorithm (21)(<http://www.cbs.dtu.dk/services/NetMHCcons/>). Alleles HLA-A*02:01, -B*27:05 and -C*01:02 were selected for screening, using standard settings of 0.5% Rank and IC50 50 nM for strong binders, and 2% Rank and IC50 500 nM for weak binders. Peptides identified as HLA-A*02:01, -B*27:05 and -C*01:02 binders were tabulated, and Mann Whitney two tailed tests performed using Prism 7 (GraphPad Inc, US) software. Anchor motifs were analysed using Seq2Logo algorithm (22) (<http://www.cbs.dtu.dk/biotools/Seq2Logo/>), using the Shannon format and standard settings.

Acknowledgements.

This work was funded by the Melville Trust for the Care and Cure of Cancer, Scotland, UK.

Conflict of interest

The authors declare no conflicts of interest.

Authorship Contributions.

SJP and CB designed and obtained the funding for the study. SJP and FGMC isolated the peptides. SAS and SLS performed the mass spectrometry and data analysis. SJP performed the MHC algorithm data. ANA and SJP wrote the first draft of the manuscript, with all authors contributing to the final version.

References.

1. Costa-Silva, B., Aiello, N. M., Ocean, A. J., Singh, S., Zhang, H., Thakur, B. K., Becker, A., Hoshino, A., Mark, M. T., Molina, H., Xiang, J., Zhang, T., Theilen, T. M., Garcia-Santos, G., Williams, C., Ararso, Y., Huang, Y., Rodrigues, G., Shen, T. L., Labori, K. J., Lothe, I. M., Kure, E. H., Hernandez, J., Doussot, A., Ebbesen, S. H., Grandgenett, P. M., Hollingsworth, M. A., Jain, M., Mallya, K., Batra, S. K., Jarnagin, W. R., Schwartz, R. E., Matei, I., Peinado, H., Stanger, B. Z., Bromberg, J., and Lyden, D. (2015) Pancreatic cancer exosomes initiate pre-metastatic niche formation in the liver. *Nat Cell Biol* **17**, 816-826
2. Arakelyan, A., Fitzgerald, W., Zicari, S., Vanpouille, C., and Margolis, L. (2017) Extracellular Vesicles Carry HIV Env and Facilitate Hiv Infection of Human Lymphoid Tissue. *Sci Rep* **7**, 1695
3. Todorova, D., Simoncini, S., Lacroix, R., Sabatier, F., and Dignat-George, F. (2017) Extracellular Vesicles in Angiogenesis. *Circulation research* **120**, 1658-1673
4. Denzer, K., van Eijk, M., Kleijmeer, M. J., Jakobson, E., de Groot, C., and Geuze, H. J. (2000) Follicular dendritic cells carry MHC class II-expressing microvesicles at their surface. *J Immunol* **165**, 1259-1265
5. Thery, C., Zitvogel, L., and Amigorena, S. (2002) Exosomes: composition, biogenesis and function. *Nature reviews. Immunology* **2**, 569-579
6. Whiteside, T. L. (2017) Exosomes carrying immunoinhibitory proteins and their role in cancer. *Clin Exp Immunol*
7. Syn, N. L., Wang, L., Chow, E. K., Lim, C. T., and Goh, B. C. (2017) Exosomes in Cancer Nanomedicine and Immunotherapy: Prospects and Challenges. *Trends in biotechnology*
8. Marino, J., Babiker-Mohamed, M. H., Crosby-Bertorini, P., Paster, J. T., LeGuern, C., Germana, S., Abdi, R., Uehara, M., Kim, J. I., Markmann, J. F., Tocco, G., and Benichou, G. (2016) Donor exosomes rather than passenger leukocytes initiate alloreactive T cell responses after transplantation. *Science immunology* **1**
9. Lundberg, V., Berglund, M., Skogberg, G., Lindgren, S., Lundqvist, C., Gudmundsdottir, J., Thorn, K., Telemo, E., and Ekwall, O. (2016) Thymic exosomes promote the final maturation of thymocytes. *Sci Rep* **6**, 36479
10. Lynch, S., Santos, S. G., Campbell, E. C., Nimmo, A. M., Botting, C., Prescott, A., Antoniou, A. N., and Powis, S. J. (2009) Novel MHC class I structures on exosomes. *J Immunol* **183**, 1884-1891
11. Soo, C. Y., Song, Y., Zheng, Y., Campbell, E. C., Riches, A. C., Gunn-Moore, F., and Powis, S. J. (2012) Nanoparticle tracking analysis monitors microvesicle and exosome secretion from immune cells. *Immunology*
12. Zheng, Y., Campbell, E. C., Lucocq, J., Riches, A., and Powis, S. J. (2013) Monitoring the Rab27 associated exosome pathway using nanoparticle tracking analysis. *Experimental cell research* **319**, 1706-1713
13. Admyre, C., Johansson, S. M., Paulie, S., and Gabrielsson, S. (2006) Direct exosome stimulation of peripheral human T cells detected by ELISPOT. *Eur J Immunol* **36**, 1772-1781
14. Hassan, C., Kester, M. G., de Ru, A. H., Hombrink, P., Drijfhout, J. W., Nijveen, H., Leunissen, J. A., Heemskerk, M. H., Falkenburg, J. H., and van Veelen, P. A. (2013) The human leukocyte antigen-presented ligandome of B lymphocytes. *Mol Cell Proteomics* **12**, 1829-1843
15. Gercel-Taylor, C., Atay, S., Tullis, R. H., Kesimer, M., and Taylor, D. D. (2012) Nanoparticle analysis of circulating cell-derived vesicles in ovarian cancer patients. *Analytical biochemistry* **428**, 44-53
16. Navabi, H., Croston, D., Hobot, J., Clayton, A., Zitvogel, L., Jasani, B., Bailey-Wood, R., Wilson, K., Tabi, Z., Mason, M. D., and Adams, M. (2005) Preparation of

- human ovarian cancer ascites-derived exosomes for a clinical trial. *Blood cells, molecules & diseases* **35**, 149-152
17. Bassani-Sternberg, M., Braunlein, E., Klar, R., Engleitner, T., Sinitcyn, P., Audehm, S., Straub, M., Weber, J., Slotta-Huspenina, J., Specht, K., Martignoni, M. E., Werner, A., Hein, R., D. H. B., Peschel, C., Rad, R., Cox, J., Mann, M., and Krackhardt, A. M. (2016) Direct identification of clinically relevant neoepitopes presented on native human melanoma tissue by mass spectrometry. *Nat Commun* **7**, 13404
 18. Pitt, J. M., Andre, F., Amigorena, S., Soria, J. C., Eggermont, A., Kroemer, G., and Zitvogel, L. (2016) Dendritic cell-derived exosomes for cancer therapy. *J Clin Invest* **126**, 1224-1232
 19. Caron, E., Kowalewski, D. J., Chiek Koh, C., Sturm, T., Schuster, H., and Aebersold, R. (2015) Analysis of Major Histocompatibility Complex (MHC) Immunopeptidomes Using Mass Spectrometry. *Mol Cell Proteomics* **14**, 3105-3117
 20. Fortier, M. H., Caron, E., Hardy, M. P., Voisin, G., Lemieux, S., Perreault, C., and Thibault, P. (2008) The MHC class I peptide repertoire is molded by the transcriptome. *J Exp Med* **205**, 595-610
 21. Karosiene, E., Lundegaard, C., Lund, O., and Nielsen, M. (2012) NetMHCcons: a consensus method for the major histocompatibility complex class I predictions. *Immunogenetics* **64**, 177-186
 22. Thomsen, M. C., and Nielsen, M. (2012) Seq2Logo: a method for construction and visualization of amino acid binding motifs and sequence profiles including sequence weighting, pseudo counts and two-sided representation of amino acid enrichment and depletion. *Nucleic Acids Res* **40**, W281-287

Figure Legends

Table 1. Peptide identification and predicted binding affinities. The sequence of the identified peptides for cell and EV derived peptides eluted from HLA-A*02:01 and HLA-B*27:05 are shown in alphabetical order. Peptides in red are those detected in the EV pool only. Predicted binding affinities were generated using NetMHCcons 1.1.

Figure 1. Characterisation of Jesthom EV. A, Cell lysates and EVs from Jesthom cells were immunoblotted for MHC class I (HC10), GRP78, CD9 and CD81. B, representative nanoparticle tracking analysis of culture supernatant from Jesthom cells, post 0.2 μm filtration, but prior to ultracentrifugation. C, Coomassie blue stained SDS-PAGE gel of approximately 2% of the washed W6/32 immunoisolation beads. Control beads (ctrl) received just lysis buffer. The W6/32 was not cross-linked and elutes from the beads with the MHC class I. D, Immunoblot of approximately 2% of the washed W6/32 immunoisolation beads, using anti HLA-B and -C antibody HC10. The second stage anti-IgG also recognises the IgH and IgL from W6/32 used in the immunoisolation step as indicated in C.

Figure 2. Analysis of eluted HLA-A*02:01 and HLA-B*27:05 binding peptides. A and C, plot of predicted binding affinities (using NetMHCcons 1.1) for the cell and EV derived pools from HLA-A*02:01 and HLA-B*27:05. Data are shown as mean plus SEM (shown in red). Mann Whitney tests indicated no significant differences. B and D, plots of the peptide lengths, shown as a percentage of the whole pool for HLA-A*02:01 and HLA-B*27:05. E and F, Peptide anchor binding motifs (using Seq2Logo) for the 9 mer, 10 mer and 11 mer peptides from each of the cell and EV derived pools from HLA-A*02:01 and HLA-B*27:05.

B27 cells	nM	B27 EV	nM	A2 cells	nM	A2 EV	nM
ARFLTTGF	36.12	ARFLTTGF	36.12	AIAPIIAAV	13.2	AIAPIIAAV	13.2
ARFLLEGQVF	123.99	ARFPETPAF	277.63	AISGIIMGI	107.14	AIVDKVPSV	15.45
ARFPETPAF	277.63	ARFSPDGQYL	143.49	AIVDKVPSV	15.45	ALADGVQKV	8.2
ARFSPDGQYL	143.49	ARIALLPLL	34.77	ALAAALAH	17.88	ALAGHQDGITFI	24.2
ARIALLPLL	34.77	ARIPLNPVL	122.66	ALADGVQKV	8.2	ALDSQVPKV	13.42
ARIFQFQNF	361.9	ARLFIFETF	113.1	ALDSQVPKV	13.42	ALDTHVHDPV	38.54
ARIPLNPVL	122.66	ARLKEVLEY	302.73	ALFQRPLI	53.61	ALLAYTLGV	5.1
ARLFIFETF	113.4	ARLQTALLV	89.62	ALIEKLEVEL	6.06	ALLDRIVSV	3.8
ARLKEVLEY	302.73	ARNKAITSL	147.43	ALLAYTLGV	5.1	ALMDEVVKA	7.6
ARLPLVNSY	113.71	ARNPPVSK	243.82	ALMPVLNQV	4.52	ALMPVLNQV	4.52
ARLQTALLV	89.62	ARSPVAPAR	306.02	ALPPLTTV	12.71	ALSDSIHTV	4.26
ARLTDYVAF	330.1	ARTPVMSTY	432.64	ALSDSIHTV	4.26	ALWDIETGQQTV	6.4
ARNKAITSL	147.43	ARVSIVNQY	307.68	ALTSVVVTL	41.35	AMWEHPITA	9.34
ARNLIYFGF	130.88	ARVYLNQDGM	487.32	ALWDIETGQQTV	6.4	FASHVSPEV	27.71
ARNPPGF	418.82	ERLQYVFGY	261.59	AMFDHIPVGV	3.89	FIYHGEVPA	53.03
ARSPVAPAR	306.02	GRAFIFPSY	78.29	AMRLRIPSL	10.46	FLANIGTSV	6.4
ARSSVTVAV	540.07	GRAPISNPGM	253.23	AMPPPPQGV	323.04	FLDGNEMTL	14.55
ARTPVMSTY	432.64	GRFGSGMNM	84.85	AMWEHPITA	9.34	FLEKLLPPV	4.04
ARTPVTSTY	605.05	GRFSGLLGR	35.73	AQLENPAAV	33.3	FLNNQEYVL	19.81
ARVKMQVTM	153.95	GRHAVVVGR	73.37	FASHVSPEV	27.71	FLQEKSPAV	3.74
ARVSIVNQY	307.68	GRIANTYNL	91.09	FIDEYVETV	4.13	FMTATIAEGL	9.65
ARVYLNQDGM	487.32	GRIDKPILK	198.52	FIIQGLRSV	15.12	FVLPPELPSV	4.75
ARYGSSNI	270.22	GRIGQAIAR	142.72	FIMIKNLLL	42.94	GLAAGGIVAV	21.37
ERLQYVFGY	261.59	GRIKAIQLEY	98.79	FLADPSAFVAA	31.72	GLAPKPVQV	40.9
FRLFPVPGSGL	106.56	GRILSGVVTM	132.31	FLDPRPLTVV	9.6	GLATDVQTV	24.07
GRAFLKRKEY	340.99	GRIVTIFAF	74.97	FLDSTSPLL	4.43	GLIDRQVTV	10.81
GRAPISNPGM	253.23	GRLGLVTSR	43.65	FLEKLLPPV	4.04	GLMTTVHAI	10.3
GRASPPPTY	495.29	GRNSFEVRV	1050.6	FLLALEPEL	3.57	GLNEEIARV	14.55
GRFGGNPGGF	81.75	GRSEIYNY	265.87	FLLDEGRIT	230.98	GLSTEGIYRV	24.73
GRFGSGMNM	84.45	GRSSVFSSR	267.31	FLLPILSQI	5.74	GLWEIENNPTV	21.03
GRFSSTGLFY	220.01	GRTFIQPNM	249.16	FLSEEGGHVAV	24.87	GQIEVPEV	4.15
GRHAVVVGR	73.37	GRTNLIVNY	133.75	FLSELTQQL	5.01	HIENIVAV	18.17
GRHGVFLEL	71.79	GRVFIKSY	147.43	FLSTINVGL	7.6	HLLLEPIYL	7.6
GRIDKPILK	198.52	GRVGTVIGSNK	531.38	FLYTGEDTV	16.22	HLSIINEYL	138.16
GRIGVITNR	138.91	GRVGVITNR	222.4	FMFDFGDGEIFHV	2.52	ILDQKINEV	13.42
GRIKAIQLEY	98.79	GRYAGGQGY	80.87	FMLPDPQNISL	14.4	ILTDADPEV	10.07
GRILSGVVTM	132.31	GRYPGSVNY	193.22	FVFSFPVSV	4.62	ILTDITKGV	37.71
GRIPGIYGR	90.11	HRAQVIYTR	54.48	FVLPPELPSV	4.75	IMLEALERV	5.38
GRIVTIFAF	74.97	HRFEQAFYTY	47.34	GIFGGHIRSV	99.86	ITYSQLITL	312.72
GRLAHEVGWY	129.48	HRFYGKNSSY	122	GLADNTVIAKV	24.33	KIYEQVEV	7.81
GRMEGPPPTY	95.63	HRLPPVTSF	98.79	GLAPKPVQV	40.9	KLDQDLNEV	11.05
GRNSFEVRV	1050.6	HRYGDGGSTF	107.72	GLATDVQTV	24.07	KLFGMIITI	8.07

GRSAFIGIGF	107.14	IRAAPPLF	243.82	GLDGPPTV	51.34	KLHGVNINV	16.84
GRSEVIYNY	265.87	IRLPSQYNF	291.48	GLDRNAPSV	59.73	KLLDPEDVAVQL	24.73
GRTEVSFTL	212.98	IRNAHSIHQR	471.75	GLIDRQVTV	10.81	KLSGSLVAKL	54.48
GRTFIQPNM	249.16	KRFEELTNL	111.88	GLIGVGLINV	18.87	LLDSAPLNV	20.14
GRTNLIVNY	133.75	KRFEQEINAKK	170.61	GLLGNVAEV	8.2	LLDVPTAAV	28.78
GRVALADIAF	254.61	KRFKEANF	234.76	GLSQVAVTV	44.6	LLGPPVGV	72.97
GRVFIKSY	147.43	KRFQVAVNL	37.71	GLWEIENPTV	21.03	LLIENVASL	8.34
GRVGTVIGSNK	531.38	KRIKPRPERF	87.7	GLWGQSVPTA	51.06	LLLDVPTAAV	7.73
GRVGVITNR	222.4	KRLASSVLR	54.19	GQIEVVPEV	4.15	LLPPAPPHA	245.15
GRWPGSSLY	54.78	KRLDINTNTY	134.47	HIIENIVAV	18.17	LMDHTEV	3.8
GRWQPLIY	37.71	KRLSKVUNI	115.57	HLLEPIYL	7.6	LMVDHVTEV	3.55
GRYAGQGY	80.87	KRNPGVKEGY	484.69	HLSIINEYL	138.16	MLPPPPLTA	263.01
GRYPGVSNY	193.22	KRWQGGERSM	31.38	ILDKKVEKV	75.79	QLSEVFIQL	23.94
GRYQVSWSL	34.77	KRYKSIVKY	71.79	ILDQKINEV	13.42	QLVDIIEKV	21.25
HRAQVIYTR	54.48	LRFQSSAVM	270.22	ILDVTVVYL	31.89	RLIQESPTL	50.51
HRDSHITNL	1091.15	LRNPLIAGK	110.08	ILTDITKGV	37.71	RLNEAAVTV	16.31
HRFEQAFYTY	47.34	LRNQSVFNF	522.82	ILTETINTV	11.98	RLPEAIEEV	8.52
HRFYGKNSSY	122	NRFAGGIGL	83.54	IMLEALERV	5.38	RLQEDPPAGV	44.6
HRIKDYHSY	253.23	QRAAVIERF	189.08	IQDNHDGTYTV	409.85	RLQEDPPVGV	42.25
HRITIKKRF	211.83	QRFLSFGF	50.78	KIGTYFRV	212.98	RLQEEINEV	9.91
HRLPPVTSF	98.79	QRNEVVVEL	759.4	KIYEQVEV	7.81	SIIGRLLEV	18.27
HRNEVTVEL	388.27	QRQDIAFAY	337.32	KLADFGDAVQL	52.18	SLADLQNDV	35.34
HRYGDGGSTF	107.72	QRTDVLTL	719.41	KLAENIDAQL	26.25	SLAEVAGLQV	35.15
IRAAPPLF	243.82	RRFSPIPPLSY	26.25	KLDQDLNEV	11.05	SLAQYLINV	4.65
IRLPSQYNF	291.48	RRFTEIYEF	18.47	KLFGMIIT	8.07	SLAQYNPKL	20.47
IRNAHSIHQR	471.75	RRFVNVVPTF	14.55	KLGSVPVTV	21.96	SLAVADLTFV	17.59
KRAALQALK	27.71	RRFVNVVPTFGK	14.48	KLIDGQVIQL	11.66	SLDQPTQTV	91.58
KRFADEGTVVKR	74.57	RRIKEIVKKH	104.28	KLIPQLPTL	6.03	SLHDIQLSL	24.47
KRFEHSACL	54.48	RRISGVDRYY	66.56	KLLDISELDMV	9.81	SLINVLISV	11.47
KRFEQEINAKK	170.61	RRLALFPGVA	32.77	KLLDPEDVAVQL	24.73	SLLDPVEV	3.31
KRFGKAYNL	22.56	RRGLALGL	9.39	KLLQFYPSL	6.94	SLLDRFLATV	5.8
KRFKEANF	234.76	RRLPDVVTGY	133.03	KLNPQQFEV	6.71	SLLLENLEKI	21.03
KRFKVSDEVGF	260.18	RRSELLRY	38.33	KLYAGAILEV	4.67	SLLLEVNEESTV	27.11
KRFQVAVNL	37.71	RRLSYNTASNK	67.28	KVLGIVVGV	13.13	SLLGGDVSV	9.49
KRHNYVRKV	149.84	RRMGPPVGGHR	67.65	LLDRFLATV	9.54	SLLPEGPAI	28.47
KRIDIIHNL	46.57	RRMGPPVGGHRR	21.49	LLDVPTAAV	28.78	SLLPPDALVGL	51.89
KRLDINTNTY	134.47	RRNGTLPWLR	28.62	LLGPPVGV	72.97	SLLQTLKYV	6.75
KRLDVTQVSF	60.71	RRNPYFRNK	55.08	LLIDDKGTIKL	84.9	SLMLVTVEL	12.51
KRLGLTVTY	44.12	RRSDVEILGY	90.6	LLIENVASL	8.34	SLSPIYPAA	41.12
KRMNPNPSITY	81.75	RRSKEITVR	141.18	LLIPGLATA	13.57	SLWGQPAEA	51.61
KRNDYVHAL	69.88	RRVNTTQKRY	102.05	LLISGLPTI	5.87	SLYDYNPNL	3.43
KRNPGVKEGY	484.69	SRFLMPEAY	192.18	LLLDVPTAAVQA	32.59	SMADIPLFGV	16.39
KRQAIKTAF	98.79	SRIHPVSTM	236.04	LLMLDVMII	37.51	SMSADVPLV	5.47
KRTSIETNV	995.27	SRLAHYNKR	328.32	LLPEGPAI	25.55	SVIEQIVYV	6.06

KRYAVPSAGL	33.48	SRLGLPLLL	31.38	LLPPAPPHA	245.15	TLFDYEVRL	8.57
KRYKSIVKY	71.79	SRNEGVATY	1229.06	LMDHITPEV	3.8	TLWVDPYEV	6.4
LRFEVWPSKF	95.12	SRTSVQPTF	437.34	LMVDHVTEV	3.55	TLYEAVREV	11.17
LRFQSSAVM	270.22	SRTVVYITY	700.21	MLFPGSIAL	4.78	TVLFPVSTV	40.68
LRNPLIAGK	110.08	SRVKLILEY	166.06	MLPPPPLTA	263.01	VLIDYQRNV	11.53
LRNQSVFNF	522.82	SRYQGVNLY	181.07	MLYDIVPVV	2.78	VLIEGSINSV	6.43
NRFAGFGIGL	83.54	TRYQGVNLY	384.09	NLASFIEQV	10.87	VLIETLVTL	10.75
NRLPLVVSF	141.95	YRFLPQKIYL	63.39	NLIDLDDLIV	11.6	VLIPKLPQL	10.75
QRAAVIERF	189.08			NLLPKLHIV	17.21	VMSKIVQV	10.46
QRFPLSFGF	50.78			NMVAKVDEV	57.51	YLADVTNAL	3.51
QRHSFQISL	105.42			QLLDQVEQI	53.32	YLDPAQRGV	24.87
QRIDLAVLL	116.83			QLLEKVP TL	11.41	YLGDVSERV	7.24
QRIYLVTTY	175.29			QLVDIIEKV	21.25	YLLPAIVHI	3.76
QRNEVVVEL	759.4			QVFPGLLERV	188.06	YLLTHPPPIM	31.89
QRQDIAFAY	337.32			RLFDQAFGL	4.02	YLPEDFIRV	3.99
QRTDVL TGL	719.41			RLIEESVTV	6.82	YLTNEGIQYL	11.6
QRVSIFFDY	595.31			RLLDYVUNI	3.74	YLYCTFISL	5.35
QRYPNPYSK	89.62			RLLIEDPYL	4.02	YQVGQLYSV	3.72
RQTGIVLNR	187.05			RLMNETTAV	6.94	YTSVNPNAV	33.3
RRAKLKADRY	71.41			RLPEAIEEV	8.52		
RRAQLQYVQR	34.59			RLQEDPPAGV	44.6		
RRDVQKV VGF	207.3			RLQEDPPVGV	42.25		
RRFFPYVYV	41.8			RLQEEINEV	9.91		
RRFSPIPPPLSY	26.25			RLWGEPVNL	30.54		
RRFVNVVPTF	14.55			RLYPWGVVEV	6.5		
RRIKEIVK KH	104.28			RQLEEEGITFV	64.08		
RRISGVDRYY	66.56			RVFENIVAV	10.07		
RRLPSDVVTGY	133.03			RVIGTLEEV	48.11		
RRMGPPVGGH	44.6			RVLDPMSVILEV	47.34		
RRMGPPVGGHR	67.65			SIIGRLLEV	18.27		
RRMGPPVGGHRR	21.49			SILEDPPSI	64.43		
RRWLPAGDAL	16.22			SLAEVAGLQV	35.15		
RRYFGGTEDRL	90.6			SLAQYLINV	4.65		
SRAKVKFNV	917.7			SLAQYNPKL	20.47		
SRFLMPEAY	192.18			SLDQPTQTV	91.58		
SRFQGTLYL	56.28			SLHDIQLSL	24.47		
SRFSLENNF	361.9			SLINVLISV	11.47		
SRIPFNQALVF	331.89			SLLDPVPEV	3.31		
SRLAHYNKR	328.32			SLLDRFLATV	5.8		
SRLATLNEK	198.52			SLLLENLEKI	21.03		
SRLGLPLLL	31.38			SLLVNEESTV	27.11		
SRLPSLGAGF	197.45			SLLGGDVVSV	9.49		
SRLSIPTYGL	60.06			SLLPEGPPAI	28.47		
SRLYIAYQF	52.74			SLLPPDALVGL	51.89		

SRNAQTFGF	191.14			SLQTLYKV	6.75		
SRNEGVATY	1229.06			SLMLVTVEL	12.51		
SRNGVITQY	405.44			SLPDFGISYV	6.22		
SRNSNTVVFVK	723.31			SLSPIYPAA	41.12		
SRSNTQPGF	543			SLSQTPPRV	75.79		
SRTSVQPTF	437.34			SLWGQPAEA	51.61		
SRVKLILEY	166.06			SLYDYNPNL	3.43		
SRWEKVQR	93.59			SLYGGTITI	19.28		
SRYQGVNLY	181.07			SMADIPLGFGV	16.39		
TRIQNPSAYAK	979.25			SMSADVPLV	5.47		
TRSGAIFTK	238.6			SMYDKVLMML	10.58		
TRYQGVNLY	384.09			SQTFVNPHV	358.01		
VRFYIESISY	267.31			SVIEQIVYV	6.06		
YRFFLGNQF	42.71			TLFDYEVRL	8.57		
YRLGNVDAFQL	61.37			TLIEDILGV	4.36		
				TLIGLSIKV	15.61		
				TLWVDPYEV	6.4		
				TYEAVREV	11.17		
				VLFENTDSVHL	21.72		
				VLIDVGTGYV	10.07		
				VLIDYQRNV	11.53		
				VLEGSINSV	6.43		
				VLIPKLPQL	10.75		
				VLLDAPIQL	8.43		
				VLLGKVVVV	6.43		
				VLMTEDIKL	54.78		
				VLQDIQVML	21.72		
				VLWDRTFSL	3.43		
				VMDSKIVQV	10.46		
				YLADVTNAL	3.51		
				YLGQVTTI	52.74		
				YLIEPDVEL	5.99		
				YLLDQHILI	4.4		
				YLLEQTPEQQA	25.55		
				YLLPAIVHI	3.76		
				YLLQEPPTV	13.57		
				YLPEDFIRV	3.99		
				YLSKIIPAL	4.29		
				YLTHDSPSV	5.29		
				YLTNEGIQYL	11.6		
				YLYPDITRL	4.06		
				YQVGQLYSV	3.72		

Table 1.

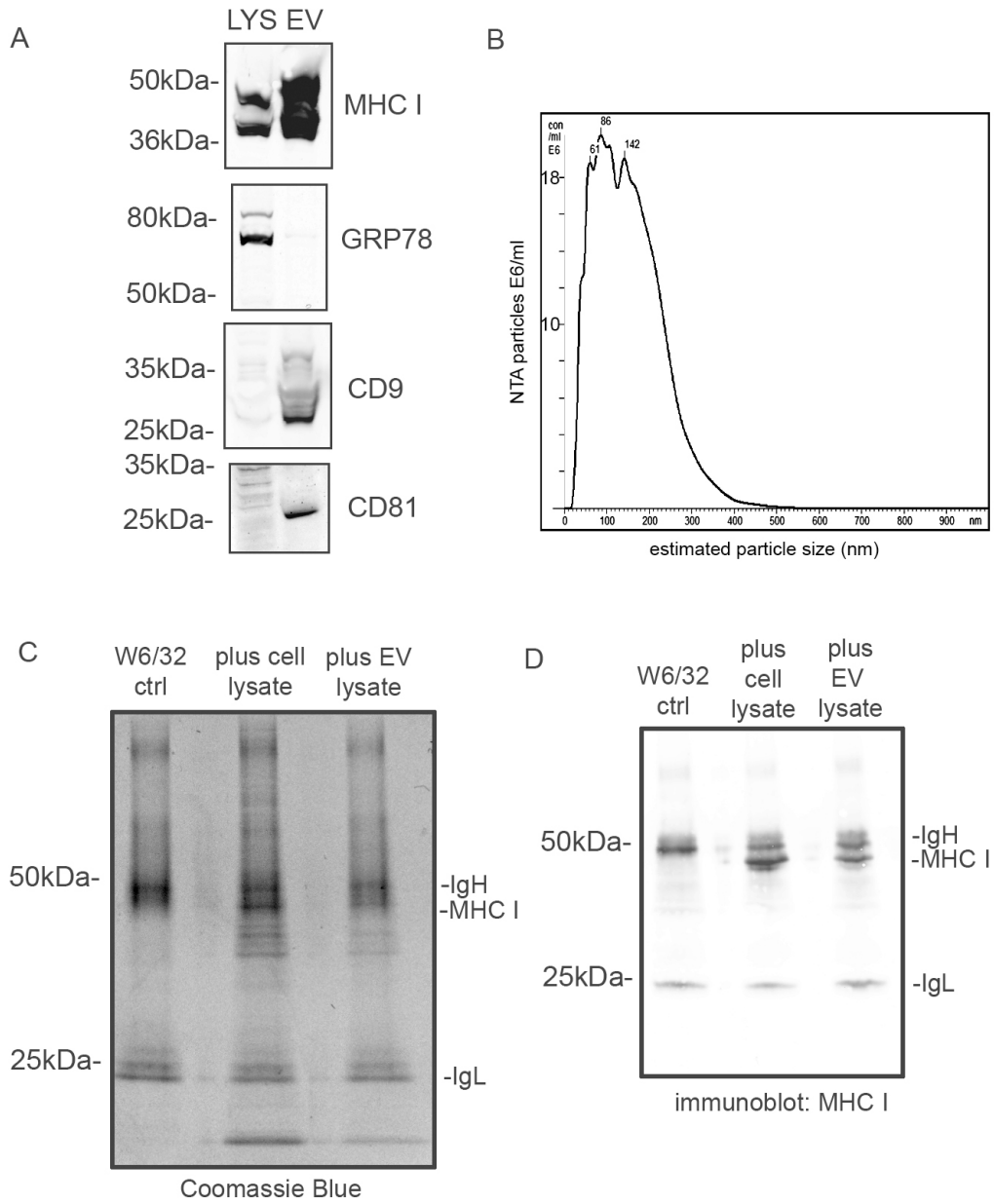


Figure 1

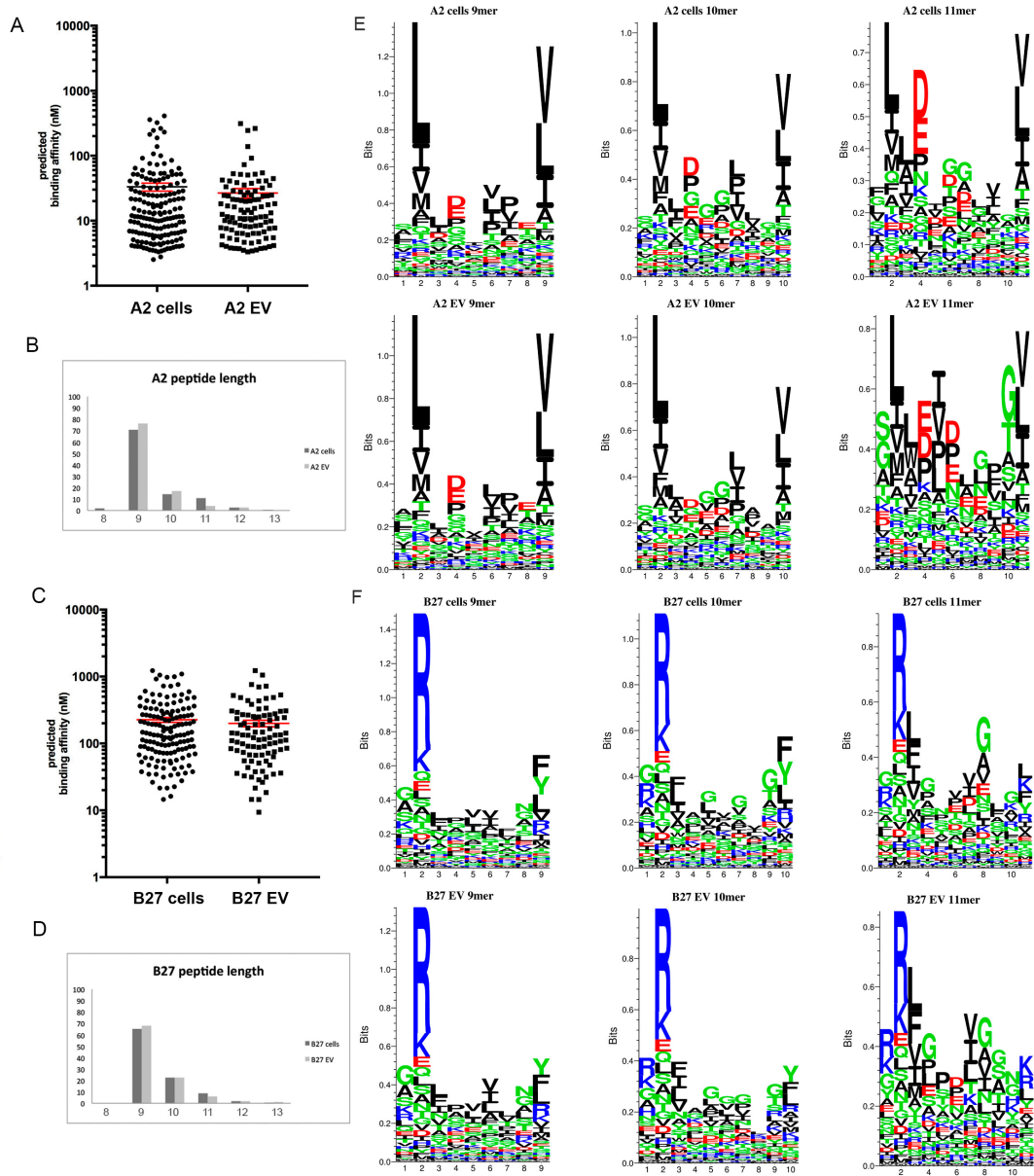


Figure 2